SNORD11B-mediated 2'-O-methylation of primary let-7a in colorectal carcinogenesis

Qiuhui Pan (panqiuhui_med@163.com)
Shanghai Children's Medical Center, School of Medicine, Shanghai Jiaotong University
Zhixuan Bian
Chang Xu
Xiaoying Wang
Yan Chen
Siwei Mao
Qi Wu
Jiabei Zhu
Nan Huang
Yue Zhang
Ji Ma
Fenyong Sun

Article

Keywords: Colorectal cancer, snoRNAs, 2'-O-methylation, primary miRNA maturation, let-7

Posted Date: March 1st, 2023

DOI: https://doi.org/10.21203/rs.3.rs-2621336/v1

Version of Record: A version of this preprint was published at Oncogene on August 24th, 2023. See the published version at https://doi.org/10.1038/s41388-023-02808-1.

Abstract

Evidence indicates that small nucleolar RNAs (snoRNAs) participate in tumorigenesis and development and could be promising biomarkers for colorectal cancer (CRC). Here, we examine the profile of snoRNAs in CRC and find that expression of SNORD11B is increased in CRC tumor tissues and cell lines, with a significant positive correlation between SNORD11B expression and that of its host gene NOP58. SNORD11B promotes CRC cell proliferation and invasion and inhibits apoptosis. Mechanistically, SNORD11B promotes the processing and maturation of 18S ribosomal RNA (rRNA) by mediating 2'-O-methylated (Nm) modification on the G509 site of 18S rRNA. Intriguingly, SNORD11B mediates Nm modification on the G225 site of MIRLET7A1HG (pri-let-7a) with canonical motif, resulting in degradation of pri-let-7a, inhibition of DGCR8 binding, reduction in mature tumor suppressor gene let-7a-5p expression, and upregulation of downstream oncogene translation. SNORD11B performs better than CEA and CA199 in diagnosing CRC. High expression of SNORD11B is significantly correlated with more advanced TNM stage and lymph node metastasis, which indicate poor prognosis.

Introduction

Colorectal cancer (CRC) is among the most common malignant tumors of the digestive system and has become the second leading cause of cancer deaths worldwide, accounting for 9.4% [1]. CRC is difficult to diagnose at an early stage and may be asymptomatic until it reaches the advanced stages. The 5-year overall survival rate for advanced CRC is only 14% [2]. The most commonly used molecular markers for CRC diagnosis and prognosis are carcinoembryonic antigen (CEA) and carbohydrate antigen 199 (CA199); however, they are both elevated in the plasma of patients with various adenocarcinomas, resulting in poor sensitivity and specificity [3]. Therefore, further investigation of the molecular mechanisms underlying the development of CRC is required to find effective interventions and early diagnostic and prognostic biomarkers, which are crucial for reducing mortality and improving prognosis of patients.

Small nucleolar RNAs (snoRNAs) are a large family of non-coding RNAs found in all eukaryotes and archaea, with a length of approximately 50–200 nucleotides (nt) [4]. snoRNAs are considered to have the specific function of regulating ribosomal RNAs (rRNAs) and small nuclear RNAs (snRNAs) by mediating nucleotide modifications of the target residues, thereby influencing biosynthesis and processing of the ribosome and spliceosome [5,6]. snoRNAs can be classified into two main families: C/D box snoRNAs (SNORDs) and H/ACA box snoRNAs (SNORAs) [7]. SNORDs and SNORAs are mainly located in the nucleolus, respectively mediating 2'-O-methylated (Nm) modification and pseudouridylation of their targets through direct base pairing in a specific manner. In this process, they interact with core chaperone proteins to enhance stability and catalytic activity [8]. snoRNAs have increasingly been found to be involved in the regulation of post-transcriptional processes, including acetylation of rRNAs [9], regulation of splicing patterns [10], and modulation of mRNA abundance and translation efficiency. Thus, they have

important roles in a variety of tumors [11,12]. However, there have been few studies of the involvement of snoRNAs are involved in the development of CRC.

MicroRNAs (miRNAs) are first transcribed from the corresponding miRNA transcription units to produce primary miRNAs (pri-miRNAs), which are subsequently processed in the nucleus by a complex containing Drosha and its co-factor DGCR8 into precursor miRNAs, followed by further processing to form mature miRNAs in the cytoplasm [13]. Various modifications have been identified on pri-miRNAs, including N6-methyladenosine, 7-methylguanosine, pseudouridylation, and adenosine-to-inosine editing, which have important roles in the regulation of pri-miRNA maturation [14]. However, no study has yet reported the existence and function of Nm modifications on pri-miRNAs.

Here, we report a SNORD, SNORD11B, that is dramatically upregulated in CRC tissues and has important biological functions. We identified and validated let-7-family miRNAs as downstream targets of SNORD11B. Taking let-7a-5p as an example, SNORD11B reduced RNA stability and inhibited DGCR8 binding by mediating Nm modification on pri-let-7a, thereby inhibiting splicing and maturation and decreasing levels of mature let-7a-5p in the cytoplasm, resulting in promotion of CRC malignancy.

Results

Profile of snoRNAs in CRC tissues and adjacent normal tissues

To ascertain whether snoRNAs were aberrantly expressed in CRC, five pairs of CRC tissues and para-tumor tissues were subjected to snoRNA sequencing using an Illumina NovaSeq PE150 platform. Clean reads were aligned to human snoRNA sequences collected from the snoDB database [15]. The Pearson correlation matrix plot indicated that snoRNA expression was highly dissimilar between tumor and normal colon tissues (Fig. S1A). A total of 423 snoRNAs were identified (Fig. 1A), among of which 36 snoRNAs were upregulated and 36 were downregulated (|fold-change|>1.5, $p < 0.05$) in CRC tumor tissues compared with adjacent normal tissues (Figs. 1B and S1B). These snoRNAs ranged in length from a few tens of nt to a few hundreds (Fig. S1C-D). Mapping all differentially expressed snoRNAs (DESs) to their chromosomal locations revealed that they were almost evenly distributed on most chromosomes (Fig. 1C). Of note, 62.50% (45/72) of these DESs were SNORDs and 34.72% (25/72) were SNORAs (Fig. 1D). As there is no functional annotation database for eukaryotic snoRNAs, in order to initially assess the functions of these snoRNAs, we performed GO (gene ontology) and KEGG (Kyoto Encyclopedia of Genes and Genomes) enrichment analysis of their host genes. GO and KEGG analysis showed that the host genes of these snoRNAs were mainly involved in translation in the cytoplasm and were mostly important components of the ribosome (Fig. 1E-F).

SNORD11B is significantly upregulated in CRC with poor prognosis

SNORD11B (snoRNA ID: URS000075ED7D) has a predicted 18S rRNA Nm modification site and was ranked second among DESs with a differential expression multiple of 3.512 ($p = 0.002$) in the sequencing results. Its host gene is NOP58 (nucleolar protein 58), which encodes a key protein involved in Nm modification. Therefore, we chose SNORD11B for further study. The 112-nt SNORD11B is located on chromosome 2, region 202291317–202291428, and is derived from intron 8 of its host gene NOP58 (Fig. 2A). SNORD11B is a classical SNORD with a conserved D box (CUGA) and C box (AUGAUGA). First, we examined the expression level of SNORD11B in 76 pairs of CRC tumor tissues and paired para-normal colon tissues and found that SNORD11B was significantly upregulated in CRC tumor tissues (Fig. 2B), consistent with the snoRNA-seq results. As SNORD11B is derived from the intron of NOP58, its high expression in CRC may be correlated with the level of NOP58. As previously reported, NOP58 is upregulated in CRC [16]. In our cohort, NOP58 was also significantly highly expressed in the 76 pairs of CRC tissues (Fig. 2C), and we found a significant positive correlation between NOP58 and SNORD11B expression in these tissues (Pearson's r = 0.2747, $p = 0.0163$) (Fig. 2D). We also examined the expression levels of SNORD11B in five CRC cell lines and normal human intestinal epithelial cells (HIEC) and found that the expression levels of SNORD11B were markedly higher in the CRC cell lines than in HIEC. SNORD11B expression was particularly high in HCT116 and HCT8 (Fig. 2I), so these two cell lines were selected for subsequent experiments.

SNORD11B is a potential diagnostic and prognostic biomarker in CRC

The receiver operating characteristic (ROC) curve and the area under curve (AUC) values showed that SNORD11B levels in tissues had diagnostic efficacy for CRC (AUC = 0.6784, $p = 0.003$) (Fig. 2E). And we collected plasma from 39 normal subjects (age 57.67 ± 14.74 years, without underlying gastrointestinal diseases) and 57 CRC patients (age 64.74 ± 11.29 years) and found that SNORD11B levels in plasma of CRC patients were notably higher than those in normal healthy subjects (Fig. 2F), and SNORD11B levels in plasma had better efficacy for CRC diagnosis compared with that in tissue (AUC = 0.8862, $p < 0.001$) (Fig. 2G). We also examined CEA and CA199 levels in the plasma of these participants and demonstrated that the diagnostic efficacy of SNORD11B was slightly better than that of CEA and obviously better than that of CA199 (Fig. S2A-C). These results suggest that SNORD11B could be used as a biomarker for CRC diagnosis.

To further analyze the correlations between SNORD11B expression and clinical characteristics of CRC patients, we downloaded SNORD11B expression data from The Cancer Genome Atlas colon adenocarcinoma collection (TCGA_COAD) from the SNORic database, as well as clinical characteristics and survival/prognosis information for TCGA_COAD patients from the UCSC Xena website. We integrated all the data and used chi-square tests or Fisher's exact tests to show that there were significant correlations of SNORD11B expression with colon cancer histology ($p = 0.035$), lymph node metastasis ($p = 0.027$), and TNM stage ($p = 0.003$) (Tables S1-2). Unfortunately, multivariate analysis by Cox proportional hazards regression model of clinical variables and overall survival showed that SNORD11B

level was not an independent prognostic risk factor (Fig. 2H). Nevertheless, the Kaplan–Meier survival curve and log-rank test analyses revealed that elevated SNORD11B expression was significantly associated with shortened overall survival ($p = 0.0234$) (Fig. 2I). We subsequently analyzed the patients included in the cohort of this study; owing to a lack of relevant data on patient prognosis, the correlation between SNORD11B and each clinical feature was assessed by chi-square test or Fisher's exact test. As shown in Tables S3-6, there were significant correlations between tissue SNORD11B levels and lymphatic invasion ($p < 0.001$) and TNM stage ($p = 0.017$), as well as plasma SNORD11B (lymphatic invasion, $p = 0.003$; TNM stage, $p < 0.001$). These results suggest that SNORD11B level could reflect poor prognosis of CRC patients to some extent and could thus serve as a potential prognostic marker.

SNORD11B promotes CRC malignant progression in vitro **and** in vivo

Aberrantly high expression of SNORD11B may have a synergistic role in the development of CRC. Therefore, to explore the biological function of this snoRNA, we designed antisense oligonucleotides (ASOs) to interfere with its expression in CRC cell lines. The knockdown efficiencies of two ASOs targeting SNORD11B were validated by real-time quantitative PCR (RT-qPCR) after transfection of HCT116 and HCT8 cells (Fig. 3A,B). As expected, Cell Counting Kit-8 (CCK8) and 5-ethynyl-2'-deoxyuridine (EdU) assays showed that the proliferation of CRC cells was significantly inhibited after SNORD11B silencing (Fig. 3C-E), and knockdown of SNORD11B abrogated the colony formation ability of CRC cells (Fig. 3F). Transwell assays showed that the invasive behavior of CRC cells was strongly reduced after SNORD11B knockdown (Fig. 3G). In addition, flow cytometry results indicated that SNORD11B silencing significantly increased early and late apoptosis levels of CRC cells (Fig. 3H-I). Conversely, the opposite results were obtained after four-fold overexpression of SNORD11B in normal colonic epithelial cells (HIEC) (Fig. S3). To further validate the pro-cancer role of SNORD11B in CRC, a xenograft tumor assay was performed. We designed three single guide RNAs (sgRNAs) targeting SNORD11B and cloned them into a LentiCRISPRv2 vector, selecting the one with the best efficiency (knockdown efficiency of about 80%) (Fig. S4A). sgSNORD11B did not affect the expression of NOP58 (Fig. S4B), so it was prioritized for further analysis. HCT116 control cells and cells with stable SNORD11B knockdown were injected subcutaneously into the left and right sides, respectively, of the rear of the axilla of 5-week-old nude mice. The weights and volumes of subcutaneous tumors in the SNORD11B-knockdown group were dramatically reduced (Fig. S4C-E) compared with controls. Immunohistochemistry analysis showed that proportions of Ki67-positive cells were significantly decreased in the SNORD11B-knockdown group (Fig. S4F). These results confirm that SNORD11B has an oncogenic role in CRC *in vivo* and *in vitro*.

SNORD11B mediates Nm modification at the G509 site of 18S rRNA

According to previous studies, 38 Nm modification sites have been reported in human 18S rRNA [17,18], and Nm modification at these sites involved the participation of SNORDs. By searching the snoRNA-related databases snOPY [19] and snoRNA Atlas [20], we found that SNORD11B had been predicted to mediate Nm

modification at the G509 site of 18S rRNA, and that SNORD11B could complementarily base-pair with sequences 5 nt upstream and 8 nt downstream of the G509 site on 18S rRNA, resulting in a stable interaction (Fig. 4A). Moreover, the G509 site is located exactly at the 5-nt position upstream of the D box of SNORD11B, consistent with the classical rules of SNORD-mediated Nm modification of target rRNAs [21]. However, no study has yet confirmed that SNORD11B can mediate Nm modification at the G509 site of 18S rRNA; therefore, an RTL-PCR (Reverse transcription at low dNTP concentrations followed by PCR) assay was performed as previously described [22]. This method provides a semi-quantitative assessment of Nm modifications between two RNA samples by comparing the PCR efficiency after RT reactions with high or low concentrations of dNTP. RT is inhibited at the Nm site under low dNTP conditions but not under standard high dNTP conditions, and the efficiency of the RT reaction can be quantified by PCR (Fig. 4B). We found that the level of the product (174 bp) of PCR with F1/R as primer was significantly increased after SNORD11B interference when the RT products obtained at a low concentration of dNTP (1 μM) were used as a template, whereas there was no difference when the RT products obtained at a high concentration of dNTP (40 μM) were used as the template (Fig. 4D), indicating that SNORD11B silencing led to increased RTL-PCR efficiency for 18S rRNA. Consistent results were obtained in cells with stable knockdown of SNORD11B via CRISPR–Cas9 (Fig. 4F), and the opposite results were observed in HIEC with SNORD11B overexpression (Fig. 4H). Previous studies have reported that Nm modification plays an integral part in rRNA precursor processing and maturation [17,23], so we designed specific primers for total 18S rRNA and its precursor (Fig. 4C). We found an elevation of immature 18S rRNA levels in CRC cells after SNORD11B interference or knockout (Fig. 4E,G) and a reduction after exogenous upregulation of SNORD11B in HIEC (Fig. 4I). We also found that levels of immature 18S rRNA were reduced in most of the CRC tumor tissues with upregulated expression of SNORD11B, of a total of 12 pairs of tissues (Fig. S5A). These results confirm that SNORD11B promotes maturation of 18S rRNA processing, and that this effect is most likely to be mediated by promotion of Nm modification at the G509 site of 18S rRNA.

Given that 18S rRNA is the core component of the small subunit of eukaryotic ribosomes and its maturation affects ribosome assembly and subsequent protein translation, we first analyzed the relative position of 18S rRNA Gm509 in the global mature ribosome structure using PyMOL software. As shown in Fig. S5B, Gm509 of 18S rRNA is far from the ribosome decoding center, which limits its effect on overall translation. To further assess the effect of SNORD11B-mediated 18S rRNA Nm modification on translation, we performed a puromycylation assay. We found that the global translation level of cells was not changed after intervention in SNORD11B expression (Fig. 4J-L). These results imply that the effect of SNORD11B on translation is limited.

SNORD11B suppresses the expression of let-7-family miRNAs

To find targets of SNORD11B other than 18S rRNA, we conducted *in silico* prediction of SNORD11B interaction factors using the RNAinter database [24]. The results revealed weak binding interactions between SNORD11B and let-7-family miRNAs in several datasets. The expression of most let-7-family miRNAs was significantly elevated after SNORD11B knockdown (Figs. 5A-B and S6A-B), whereas in HIEC

cells with SNORD11B overexpression, let-7-family miRNAs were all significantly reduced in expression (Fig. S6D). Western blots showed that the expression levels of most downstream target genes of let-7-family miRNAs were significantly reduced after SNORD11B knockdown (Figs. 5C and S6G), in contrast to the results for SNORD11B-overexpressing HIEC cells (Fig. S6H).

We then selected let-7a-5p, which was regulated by SNORD11B under different treatments with relatively high fold change, as a representative of let-7-family miRNAs for subsequent experiments. Let-7a-5p was markedly downregulated in 61 pairs of CRC tumor tissues (Fig. 5D). There was also a significant negative correlation between let-7a-5p and SNORD11B expression in these tissues (Pearson's r = − 0.4058, p = 0.0012) (Fig. 5E). If SNORD11B interacted directly with let-7a-5p, it would be expected to be localized in the cytoplasm; however, RNA fluorescence in situ hybridization (FISH) assays demonstrated that SNORD11B was located in the nucleus (Figs. 5G and S6F). We separated the cytoplasmic and nuclear fractions of HCT116, HCT8, and HIEC cells. Using U6 snRNA as the nuclear control transcript and GAPDH as the cytoplasmic control, we confirmed that SNORD11B was mainly distributed in the nucleus, whereas let-7a-5p was predominantly expressed in the cytoplasm (Figs. 5F and S5E). This demonstrated that SNORD11B did not act directly on let-7a-5p, but that it could act on the primary transcript of let-7a-5p (pri-let-7a) in the nucleus, leading to decreased levels of let-7a-5p and accelerating the malignant progression of CRC.

Nucleotides 84–94 of SNORD11B could complementarily pair with pri-let-7a (Fig. 5H). The expression of pri-let-7a was significantly elevated after SNORD11B knockdown and reduced after SNORD11B overexpression (Figs. 5I and S6I). RNA stability analysis showed that the half-life of pri-let-7a was prolonged in HCT116 and HCT8 cells after SNORD11B knockdown (Fig. 5J-K) and was shortened in HIEC cells after SNORD11B overexpression (Fig. S6J).

Taken together, these results show that SNORD11B can affect pri-let-7a stability and inhibit the expression of the tumor suppressor gene let-7a-5p to promote CRC development.

SNORD11B mediates Nm modification of pri-let-7a and inhibits splicing

Notably, we found that the region where pri-let-7a binds to SNORD11B was similar to 18S rRNA, (upstream of the D box), so we speculated that the G base on the pri-let-7a corresponding to the 5 nt upstream of the SNORD11B D box may have undergone the same Nm modification as the G509 site of 18S rRNA. We mapped this binding region to the let-7a-5p host gene, lncRNA MIRLET7A1HG (miRlet-7a-1/let-7f-1/let-7d cluster host gene), and the 220–230 nt region of MIRLET7A1HG was found to be complementarily base-paired with the 84–94 nt region of SNORD11B; moreover, Nm modification may occur at the G225 site of MIRLET7A1HG (Fig. 6A). To identify whether this site underwent Nm modification, we designed site-specific primers: MeUA-RT (3' without Nm modification site G225) and MeA-RT (3' with Nm modification site G225) (Figs. 6B and S7A) and performed RTL-qPCR experiments as described previously [22] (Fig. 6C). In HCT116 and HCT8 cells after SNORD11B knockdown, the relative levels of qPCR products in the MeUA-RT with low dNTP group were significantly increased, whereas those

in the MeA-RT group were unchanged (Figs. 6D-E and S7B-C). The opposite results were obtained in HIEC with SNORD11B overexpression (Fig. S7D). These findings strongly suggest that SNORD11B mediates Nm modification at the G225 site of MIRLET7A1HG.

For further validation, we performed FISH experiments to explore that fibrillarin (FBL), the key enzyme mediating Nm modification[8], co-localized with pri-let-7a in the nucleolus (Fig. 6G-H). We then performed RNA immunoprecipitation (RIP)-qPCR experiments to verify the binding of pri-let-7a to FBL. According to the results, anti-FBL significantly recruited pri-let-7a, and this enrichment decreased to a level comparable with that of the IgG group after SNORD11B knockdown (Fig. 6I-J), indicating that FBL interacted with pri-let-7a with the involvement of SNORD11B. As the G225 site and the SNORD11B-binding region are located in the stem-loop structure of let-7a precursor, we hypothesized that the Nm modification of this site might affect the binding of DGCR8/DROSHA to pri-let-7a, thereby inhibiting splicing and maturation. We therefore performed anti-DGCR8 RIP-qPCR and found that the binding of DGCR8 to pri-let-7a was significantly enhanced upon SNORD11B knockdown, whereas DGCR8 did not bind to SNORD11B (Fig. 6K-L).

These findings suggest that SNORD11B attenuates the binding of DGCR8 to pri-let-7a by mediating Nm modification at the G225 site, thereby inhibiting the splicing and maturation of pri-let-7a in the nucleus, decreasing the expression of mature let-7a-5p, and promoting the malignant progression of CRC.

SNORD11B promotes CRC malignancy via let-7a-5p

To further verify that SNORD11B promotes CRC malignancy by inhibiting let-7a-5p, we conducted rescue experiments. We transfected SNORD11B-knockdown HCT116 and HCT8 cells with a mimic or inhibitor against let-7a-5p to overexpress or knock down the expression of let-7a-5p in the target cells. Transfection with mimic or inhibitor did not affect the expression of SNORD11B (Figs. 7A and S8A); the transfection efficiencies are shown in Figs. 7B and S8B. SNORD11B knockdown followed by further inhibition of let-7a-5p expression partially counteracted the inhibition of cell proliferation and invasion, and suppressed the increase in apoptosis caused by SNORD11B silencing, whereas followed by further let-7a-5p overexpression exacerbated the opposite results. (Figs. 7C-J and S8CJ). We verified the expression of let-7a-5p downstream genes by western blot assay and found that simultaneous knockdown of SNORD11B and let-7a-5p expression significantly enhanced the expression of target genes compared with SNORD11B knockdown alone, which was contrary to the results for SNORD11B-knockdown and let-7a-5p-overexpressing cells (Figs. 7K-L and S8K-L). These results suggest that SNORD11B promotes the malignant progression of CRC by inhibiting let-7a-5p and subsequently enhances the expression of oncogenes downstream of let-7a-5p.

Materials And Methods

CRC patients and clinical specimens

A total of 396 CRC cases with available clinical information were included in the COAD cohort of TCGA. The SNORD11B expression dataset for these samples was downloaded from the SNORic database (http://bioinfo.life.hust.edu.cn/SNORic). Plasma samples and paired CRC tissues and adjacent para-tumor tissues of CRC patients were obtained from Shanghai Tenth People's Hospital with approval of the ethics committees and written consent of each participant. Tissue specimens were immediately snap-frozen in liquid nitrogen after surgery, and plasma samples were stored at − 80 ℃ for further assays.

Cell culture and treatment

Human CRC cell lines, including HCT8, HCT116, HT29, LoVo, and SW480, and human embryonic kidney cell line 293T were purchased from the Cell Bank of the Type Culture Collection of the Chinese Academy of Sciences (Shanghai, China). HIEC were obtained from the BeNa Culture Collection (Henan, China) with STR genotyping report. HCT8 and HCT116 cells and HIEC were routinely cultured in RPMI-1640 (Gibco, USA), HT29 cells were maintained in McCoy's 5a (Invitrogen, USA), LoVo cells were grown in Ham's F-12K (Gibco, USA), SW480 cells were cultured in L15 (Hyclone, USA), and 293T cells were cultured in Dulbecco's modified Eagle medium (Gibco, USA) with 10% fetal bovine serum (Gibco, USA) and 1% penicillin–streptomycin solution (Gibco, USA) in 37 ℃ humidified incubators with 5% CO_2. For RNA stability assays, the cells were treated with actinomycin D (10 μg/ml, Sigma, USA) for the indicated times to stop transcription.

Transfection and lentivirus construction

The ASOs used for SNORD11B knockdown were designed and synthesized by RiboBio (Guangzhou, China). ASO transfection was performed using riboFECT™ CP Reagent (RiboBio, Guangzhou, China) according to the manuals. The mimic and inhibitor for let-7a-5p were purchased from GenePharma Corporation (Shanghai, China) and were transfected with Lipofectamine 2000 (Life Technologies, USA) according to the protocols. Full-length SNORD11B sequences were cloned into a pLVX-puro vector (LV-SNORD11B) by Tsingke Biotechnology Corporation (Beijing, China) for SNORD11B overexpression. SNORD11B-targeting sgRNAs (sgSNORD11B) were designed using CRISPOR (32) and cloned into a LentiCRISPRv2 plasmid. Lentivirus was packaged by co-transfection of LV-SNORD11B or sgSNORD11B vectors with helper plasmids pMD2.G and psPAX2 into 293T cells. The medium was renewed 24 h after transfection, and the supernatant containing the virus solution was collected after 48 h, filtered, and stored at − 80°C for subsequent use. The sequences of all oligos used in this study are summarized in Table S7.

Reverse transcription at low dNTP concentrations followed by (q)PCR (RTL-(q)PCR) method

RTL-P was performed as previously described [22]. As the 2'-O-methylated nucleotide could impede the RT reaction at a low dNTP concentration, the cDNA product of the RT reaction with low dNTP concentration is expected to be shorter than that with high dNTP concentration. The cDNAs were generated from 100 ng total RNA using M-MLV reverse transcriptase (Promega, USA) in the presence of either a low (1 μM) or a

high (40 μM) level of dNTPs. To detect the Nm modification on 18S rRNAs, PCR amplification was performed using PrimeSTAR Max DNA Polymerase (R045, TaKaRa, Japan) with a mixture of three PCR primers targeting the upstream or downstream region of the specific site. The PCR products were then separated on 2.5% agarose gels and visualized using a Bio-Rad imaging system. Integrated density of the DNA bands was analyzed with ImageJ software. For detection of methylated sites on pri-let-7a, cDNAs were generated from 200 ng total RNA using a low (1 μM) or a high (40 μM) level of dNTP concentration with or without anchored RT primers (MeA-RT or MeUA-RT) that were designed to anchor the modified nucleotide as previously described [22]. The cDNAs were subsequently amplified by qPCR using TB Green™ Premix Ex Taq™ II (RR820A, TaKaRa, Japan) with specific primers. Relative expression levels under low dNTP conditions were calculated using the $2^{-\Delta\Delta Ct}$ method, with the Ct values normalized using those from the high-dNTP group as internal controls. The reaction systems and procedures for RTL-PCR are summarized in Tables S10 and 11, and the primers used are listed in Table S9.

Statistics

Statistical analyses were performed using GraphPad Prism (version 8.0) or SPSS Statistics 20.0 and are presented as mean ± SD. Unless otherwise stated, *p*-values were obtained using two-tailed Student's *t*-test or one-way or two-way analysis of variance to compare the means of independent samples. Survival curves were evaluated by Kaplan–Meier analysis (log-rank test). The correlations of SNORD11B expression with clinicopathological characteristics of CRC patients were analyzed by χ^2-test or Fisher's exact test. The diagnostic value of factors was assessed via ROC curve analysis. The association between SNORD11B expression and prognosis of CRC patients was appraised using a Cox proportional hazards regression model. All experiments were conducted in triplicate. $^*p < 0.05$, $^{**}p < 0.01$, and $^{***}p < 0.001$ were considered to indicate statistical significance.

For further detailed materials and methods, see the supplementary file.

Discussion

Recently, substantial advances have been made in understanding the dysregulation of snoRNAs in tumorigenesis [26]. In this study, for the first time, we explored the biological function of SNORD11B in CRC carcinogenesis.

During ribosome biogenesis, rRNAs' precursor transcripts undergo extensive modifications [27]. The most abundant modification is site-specific Nm modification, with up to 112 different Nm modification sites identified in the human ribosome [17]. The vast majority of these Nm modifications in eukaryotes are mediated by evolutionarily conserved snoRNPs centered on SNORDs [28–30]. SNORD11B has been predicted to have strict complementary base-pairing with 18S rRNA near the G509 site. Notably, we verified the regulatory role of SNORD11B on the G509 site of 18S rRNA by RTL-PCR. Studies have reported that SNORDs are derived almost exclusively from the introns of protein-coding genes in eukaryotes and mediate Nm modifications on a plethora of rRNAs and snRNAs [31]. The host genes of

these SNORDs usually encode proteins involved in ribosome biogenesis or related functions [32], which implies some degree of coordinated expression. Our results confirm a positive correlation between NOP58 and SNORD11B, but no feedback regulatory relationship was observed. NOP58 is one of the key structural proteins mediating Nm modification, and its high expression leads to SNORD11B upregulation, which may jointly promote modification on the G509 site of 18S rRNA. Moreover, structural analysis showed that the 18S rRNA Gm509 site was spatially distant from the decoding site in the ribosome small subunit, and although the modification of this site could regulate the maturation of the 18S rRNA precursor to some extent, it had no significant effect on the global translation level in cells. This suggests that differential modification on the G509 site via SNORD11B may have other intracellular functions.

Post-transcriptional modifications affect biological processes such as splicing, stability, and translation of mRNAs by altering base-pairing interactions as well as by recruiting or decoupling RNA-binding proteins [33]. One study showed by high-throughput sequencing that Nm modifications also occur on mRNAs. However, the detection assay was complicated and the biological role of these modification has not been verified [34]. Another study reported that internal Nm modification of mRNAs could affect mRNAs' abundance and protein levels both *in vitro* and *in vivo*[35]. Nm modifications have been found to be present at the 3' termini of mature miRNAs, where they contributed to enhancing the stability of miRNAs [36–38]; however, the presence of Nm modifications on pri-miRNAs and their possible biological functions have not been reported. Here, we found that SNORD11B could regulate the expression of let-7-family miRNAs. We propose for the first time that the G225 site of MIRLET7A1HG (pri-let-7a) can undergo Nm modification in the presence of SNORD11B and FBL, resulting in a robust decrease in the stability of pri-let-7a and in its DGCR8-binding ability, inhibiting the splicing of pri-let-7a in the nucleus and further reducing the expression of oncogenes targeted by let-7a-5p in cytoplasm. Notably, the SNORD11B-mediated Nm modification site that we identified on pri-let-7 is in a common region (GAGmGUAG) of mature let-7-family miRNAs. Given that this sequence is the most important conserved motif for let-7, the Nm modification at the indicated G site may be essential for let-7 to perform its biological function properly; however, this needs further verification.

Owing to the stable expression of snoRNAs, they can be detected in blood, plasma, urine, and other body fluids [26,39], making snoRNAs suitable as novel tumor biomarkers [40,41]. We confirmed that the expression levels of SNORD11B in plasma of CRC patients are significantly higher than those of normal healthy subjects, that its diagnostic sensitivity in CRC is much better than that of CEA and CA199. Furthermore, using TCGA data and the results of clinical studies, we showed that SNORD11B is closely associated with CRC lymph node infiltration, distant metastasis, and TNM stage, indicating that SNORD11B has crucial clinical application value as a molecular marker for CRC adjuvant diagnostic and prognostic assessment.

In summary, the results of this study reveal the characteristic expression profile of snoRNAs in CRC and confirm the role of SNORD11B as an oncogene in CRC development. SNORD11B mediates Nm modification on G509 of 18S rRNA; moreover, it mediates Nm modification of pri-let-7a so as to promote

pri-let-7a degradation and inhibit the binding of the DGCR8/DROSHA complex to pri-let-7a, thereby inhibiting splicing of pri-let-7a in the nucleus, reducing levels of let-7a-5p in the cytoplasm, and ultimately promoting the malignant progression of CRC (Fig. 8). This modifying effect may be commonly found on pri-miRNAs corresponding to let-7-family miRNAs, which would be an important addition to the classical regulatory factors of let-7 in cells reported by previous studies. In addition, SNORD11B is expected to be a novel molecular marker for CRC diagnosis and prognosis, and ASOs targeting SNORD11B represent a potential therapeutic strategy for CRC patients.

Declarations

Acknowledgments

Funding

This work was sponsored by the National Natural Science Foundation of China [NO: 81871727, 82172357], Key project of Shanghai "Science and Technology Innovation Action Plan" (22JC1402300), the Three-year Action Plan of Shanghai Shenkang Hospital Development Centre for Promoting Clinical Skills and Clinical Innovation Ability of Municipal Hospitals (SHDC2020CR2061B), the Joint Project of Pudong New Area Municipal Health Commission of Shanghai (PW2019D-10), and the Shanghai Key Laboratory of Clinical Molecular Diagnostics for Pediatrics (20dz2260900).

Author contributions

Conceptualization, Q.P. and F.S.; Methodology, Z.B. and C.X.; Clinical samples and information collection X.W., Y.C., Q.W. and N.H. Statistical Analysis, Z.B., S.M. and J.Z. Animal experiment Z.B., C.X. and Y.Z. Investigation Z.B., C.X. and J.Z. Writing-Original Draft, B.Z.; Supervision, Q.P. and F.S. All authors reviewed the manuscript.

Competing interests

The authors have declared no competing interest.

Data and materials availability

All data generated in this study are present in the paper and/or the Supplementary Files. The snoRNA-seq data have been deposited in the China National Centre for Bioinformation/Beijing Institute of Genomics, Chinese Academy of Sciences (GSA: HRA003909) and are publicly accessible at https://ngdc.cncb.ac.cn/gsa

References

1. Sung H, Ferlay J, Siegel RL, Laversanne M, Soerjomataram I, Jemal A *et al.* Global Cancer Statistics 2020: GLOBOCAN Estimates of Incidence and Mortality Worldwide for 36 Cancers in 185 Countries.

CA Cancer J Clin 2021; **71**: 209–249.

2. Bhullar DS, Barriuso J, Mullamitha S, Saunders MP, O'Dwyer ST, Aziz O. Biomarker concordance between primary colorectal cancer and its metastases. *EBioMedicine* 2019; **40**: 363–374.
3. Bagaria B, Sood S, Sharma R, Lalwani S. Comparative study of CEA and CA19-9 in esophageal, gastric and colon cancers individually and in combination (ROC curve analysis). *Cancer Biol Med* 2013; **10**: 148–157.
4. Boivin V, Faucher-Giguère L, Scott M, Abou-Elela S. The cellular landscape of mid-size noncoding RNA. *WIREs RNA* 2019; **10**. doi:10.1002/wrna.1530.
5. Bratkovič T, Božič J, Rogelj B. Functional diversity of small nucleolar RNAs. *Nucleic Acids Res* 2020; **48**: 1627–1651.
6. Dupuis-Sandoval F, Poirier M, Scott MS. The emerging landscape of small nucleolar RNAs in cell biology: Emerging landscape of small nucleolar RNAs. *Wiley Interdiscip Rev RNA* 2015; **6**: 381–397.
7. Boivin V, Deschamps-Francoeur G, Scott MS. Protein coding genes as hosts for noncoding RNA expression. *Semin Cell Dev Biol* 2018; **75**: 3–12.
8. Massenet S, Bertrand E, Verheggen C. Assembly and trafficking of box C/D and H/ACA snoRNPs. *RNA Biol* 2017; **14**: 680–692.
9. Sharma S, Yang J, van Nues R, Watzinger P, Kötter P, Lafontaine DLJ *et al.* Specialized box C/D snoRNPs act as antisense guides to target RNA base acetylation. *PLOS Genet* 2017; **13**: e1006804.
10. Falaleeva M, Pages A, Matuszek Z, Hidmi S, Agranat-Tamir L, Korotkov K *et al.* Dual function of C/D box small nucleolar RNAs in rRNA modification and alternative pre-mRNA splicing. *Proc Natl Acad Sci* 2016; **113**. doi:10.1073/pnas.1519292113.
11. Mannoor K, Shen J, Liao J, Liu Z, Jiang F. Small nucleolar RNA signatures of lung tumor-initiating cells. *Mol Cancer* 2014; **13**: 104.
12. Okugawa Y, Toiyama Y, Toden S, Mitoma H, Nagasaka T, Tanaka K *et al.* Clinical significance of SNORA42 as an oncogene and a prognostic biomarker in colorectal cancer. *Gut* 2017; **66**: 107–117.
13. Ma Y, Shen N, Wicha MS, Luo M. The Roles of the Let-7 Family of MicroRNAs in the Regulation of Cancer Stemness. *Cells* 2021; **10**: 2415.
14. Matsuyama H, Suzuki HI. Systems and Synthetic microRNA Biology: From Biogenesis to Disease Pathogenesis. *Int J Mol Sci* 2019; **21**: 132.
15. Bouchard-Bourelle P, Desjardins-Henri C, Mathurin-St-Pierre D, Deschamps-Francoeur G, Fafard-Couture É, Garant J-M *et al.* snoDB: an interactive database of human snoRNA sequences, abundance and interactions. *Nucleic Acids Res* 2020; **48**: D220–D225.
16. Wu H, Qin W, Lu S, Wang X, Zhang J, Sun T *et al.* Long noncoding RNA ZFAS1 promoting small nucleolar RNA-mediated 2'-O-methylation via NOP58 recruitment in colorectal cancer. *Mol Cancer* 2020; **19**: 95.
17. Ayadi L, Galvanin A, Pichot F, Marchand V, Motorin Y. RNA ribose methylation (2'-O-methylation): Occurrence, biosynthesis and biological functions. *Biochim Biophys Acta BBA - Gene Regul Mech*

2019; **1862**: 253–269.

18. Piekna-Przybylska D, Decatur WA, Fournier MJ. The 3D rRNA modification maps database: with interactive tools for ribosome analysis. *Nucleic Acids Res* 2007; **36**: D178–D183.
19. Yoshihama M, Nakao A, Kenmochi N. snOPY: a small nucleolar RNA orthological gene database. *BMC Res Notes* 2013; **6**: 426.
20. Jorjani H, Kehr S, Jedlinski DJ, Gumienny R, Hertel J, Stadler PF *et al.* An updated human snoRNAome. *Nucleic Acids Res* 2016; **44**: 5068–5082.
21. Lui L, Lowe T. Small nucleolar RNAs and RNA-guided post-transcriptional modification. *Essays Biochem* 2013; **54**: 53–77.
22. Dong Z-W, Shao P, Diao L-T, Zhou H, Yu C-H, Qu L-H. RTL-P: a sensitive approach for detecting sites of 2'-O-methylation in RNA molecules. *Nucleic Acids Res* 2012; **40**: e157–e157.
23. Cao P, Yang A, Wang R, Xia X, Zhai Y, Li Y *et al.* Germline Duplication of SNORA18L5 Increases Risk for HBV-related Hepatocellular Carcinoma by Altering Localization of Ribosomal Proteins and Decreasing Levels of p53. *Gastroenterology* 2018; **155**: 542–556.
24. Lin Y, Liu T, Cui T, Wang Z, Zhang Y, Tan P *et al.* RNAInter in 2020: RNA interactome repository with increased coverage and annotation. *Nucleic Acids Res* 2020; **48**: D189–D197.
25. Concordet J-P, Haeussler M. CRISPOR: intuitive guide selection for CRISPR/Cas9 genome editing experiments and screens. *Nucleic Acids Res* 2018; **46**: W242–W245.
26. Liang J, Wen J, Huang Z, Chen X, Zhang B, Chu L. Small Nucleolar RNAs: Insight Into Their Function in Cancer. *Front Oncol* 2019; **9**: 587.
27. Taoka M, Nobe Y, Yamaki Y, Sato K, Ishikawa H, Izumikawa K *et al.* Landscape of the complete RNA chemical modifications in the human 80S ribosome. *Nucleic Acids Res* 2018; **46**: 9289–9298.
28. Scott MS, Ono M, Yamada K, Endo A, Barton GJ, Lamond AI. Human box C/D snoRNA processing conservation across multiple cell types. *Nucleic Acids Res* 2012; **40**: 3676–3688.
29. Lin J, Lai S, Jia R, Xu A, Zhang L, Lu J *et al.* Structural basis for site-specific ribose methylation by box C/D RNA protein complexes. *Nature* 2011; **469**: 559–563.
30. Yang Z, Lin J, Ye K. Box C/D guide RNAs recognize a maximum of 10 nt of substrates. *Proc Natl Acad Sci* 2016; **113**: 10878–10883.
31. Dieci G, Preti M, Montanini B. Eukaryotic snoRNAs: A paradigm for gene expression flexibility. *Genomics* 2009; **94**: 83–88.
32. Hoeppner MP, White S, Jeffares DC, Poole AM. Evolutionarily Stable Association of Intronic snoRNAs and microRNAs with Their Host Genes. *Genome Biol Evol* 2009; **1**: 420–428.
33. Jiang X, Liu B, Nie Z, Duan L, Xiong Q, Jin Z *et al.* The role of m6A modification in the biological functions and diseases. *Signal Transduct Target Ther* 2021; **6**: 74.
34. Dai Q, Moshitch-Moshkovitz S, Han D, Kol N, Amariglio N, Rechavi G *et al.* Nm-seq maps 2'-O-methylation sites in human mRNA with base precision. *Nat Methods* 2017; **14**: 695–698.

35. Elliott BA, Ho H-T, Ranganathan SV, Vangaveti S, Ilkayeva O, Abou Assi H *et al.* Modification of messenger RNA by 2'-O-methylation regulates gene expression in vivo. *Nat Commun* 2019; **10**: 3401.
36. Motorin Y, Marchand V. Detection and Analysis of RNA Ribose 2'-O-Methylations: Challenges and Solutions. *Genes* 2018; **9**: 642.
37. Abe M, Naqvi A, Hendriks G-J, Feltzin V, Zhu Y, Grigoriev A *et al.* Impact of age-associated increase in 2'-O-methylation of miRNAs on aging and neurodegeneration in Drosophila. *Genes Dev* 2014; **28**: 44–57.
38. Liang H, Jiao Z, Rong W, Qu S, Liao Z, Sun X *et al.* 3'-Terminal 2'-O-methylation of lung cancer miR-21-5p enhances its stability and association with Argonaute 2. *Nucleic Acids Res* 2020; **48**: 7027–7040.
39. Wajahat M, Bracken CP, Orang A. Emerging Functions for snoRNAs and snoRNA-Derived Fragments. *Int J Mol Sci* 2021; **22**: 10193.
40. Thorenoor N, Slaby O. Small nucleolar RNAs functioning and potential roles in cancer. *Tumor Biol* 2015; **36**: 41–53.
41. Gong J, Li Y, Liu C, Xiang Y, Li C, Ye Y *et al.* A Pan-cancer Analysis of the Expression and Clinical Relevance of Small Nucleolar RNAs in Human Cancer. *Cell Rep* 2017; **21**: 1968–1981.

Figures

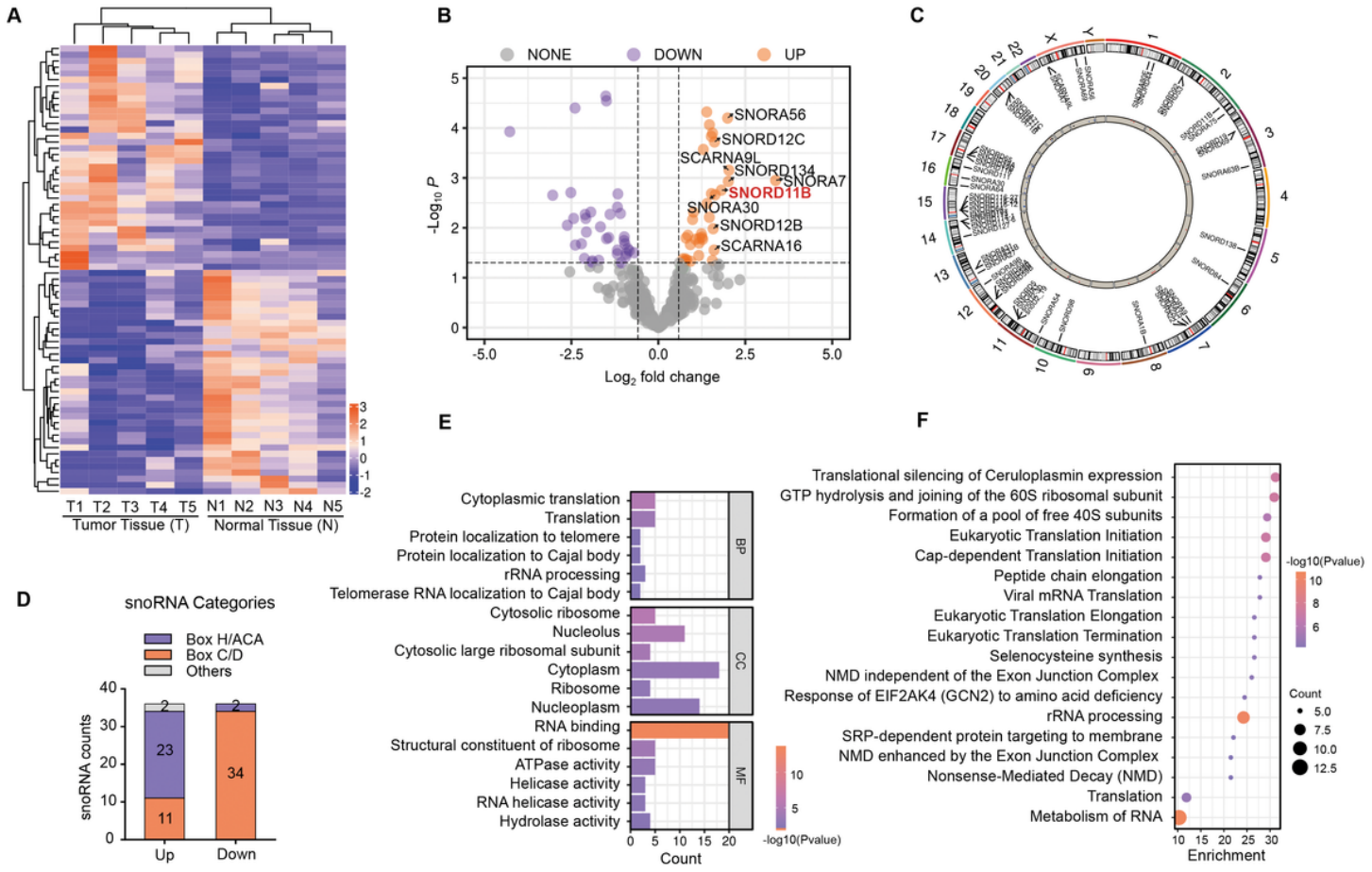

Figure 1

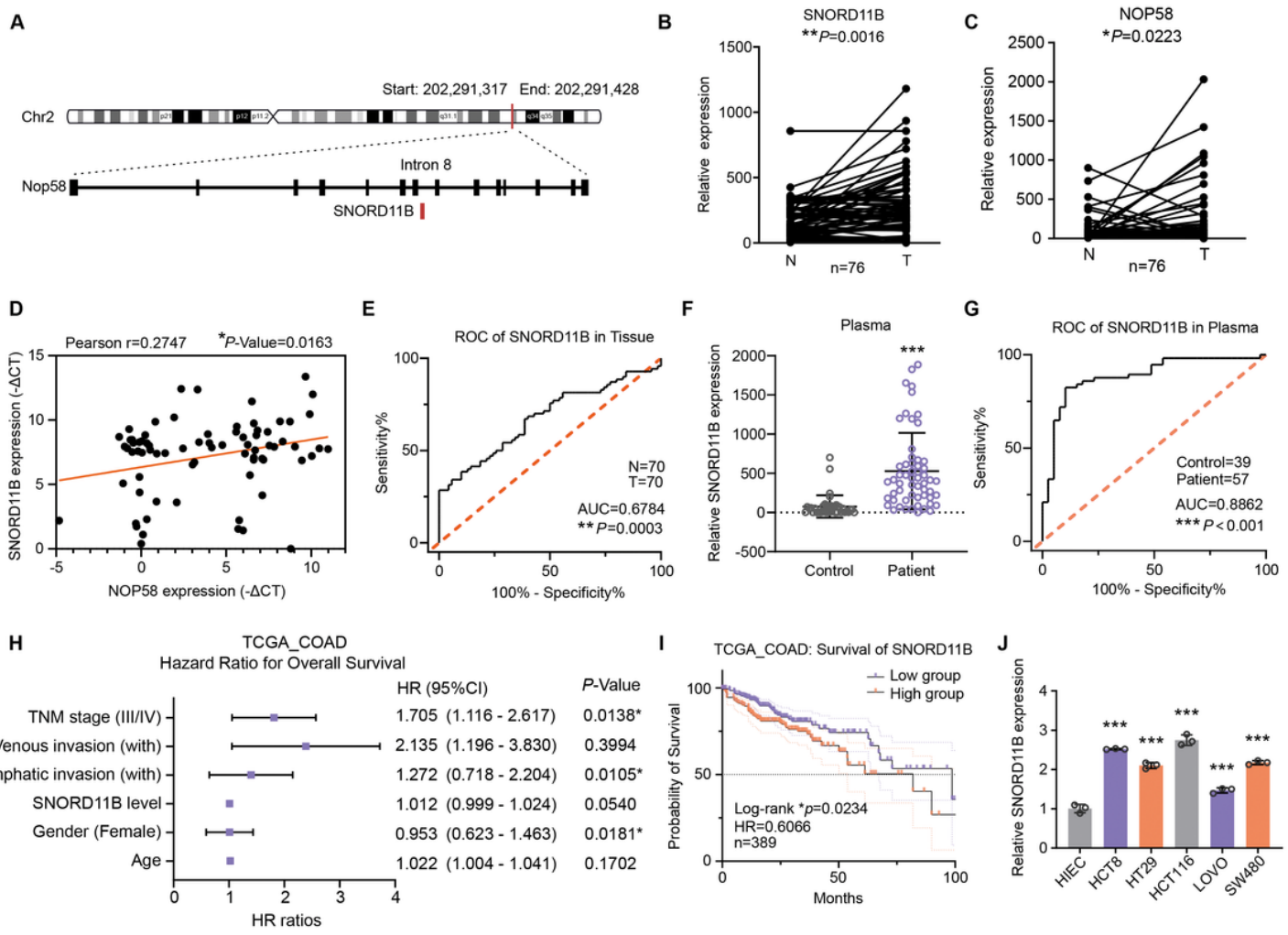

Figure 2

Identification of SNORD11B as an upregulated snoRNA in CRC. (A) Chromosome locations of SNORD11B and NOP58 according to the UCSC Genome Browser. (B–C) Expression levels of SNORD11B (B) and NOP58 (C) in paired CRC tissues (n=76) as measured by RT-qPCR. N, normal tissues; T, tumor tissues (paired-samples t-test). (D) Linear correlation analysis between SNORD11B and NOP58 expression in paired CRC tissues (Pearson's correlation analysis). (E) ROC curve for tissue-derived SNORD11B in CRC

diagnosis. (F) Expression levels of SNORD11B in plasma of CRC patients and healthy donors as detected by RT-qPCR. (G) ROC curve for plasma-derived SNORD11B in CRC diagnosis. (H) Forest plot depicting multivariate analysis of overall survival (OS) of CRC patients based on TCGA data (Cox proportional hazards regression model). (I) Kaplan–Meier analyses of correlations between SNORD11B expression levels and OS of CRC patients based on TCGA data (log-rank test). (J) Elevated expression levels of SNORD11B in normal intestinal epithelial cells (HIEC) and CRC cell lines including HCT8, HT29, HCT116, SW480, and LoVo as detected by RT-qPCR assays.

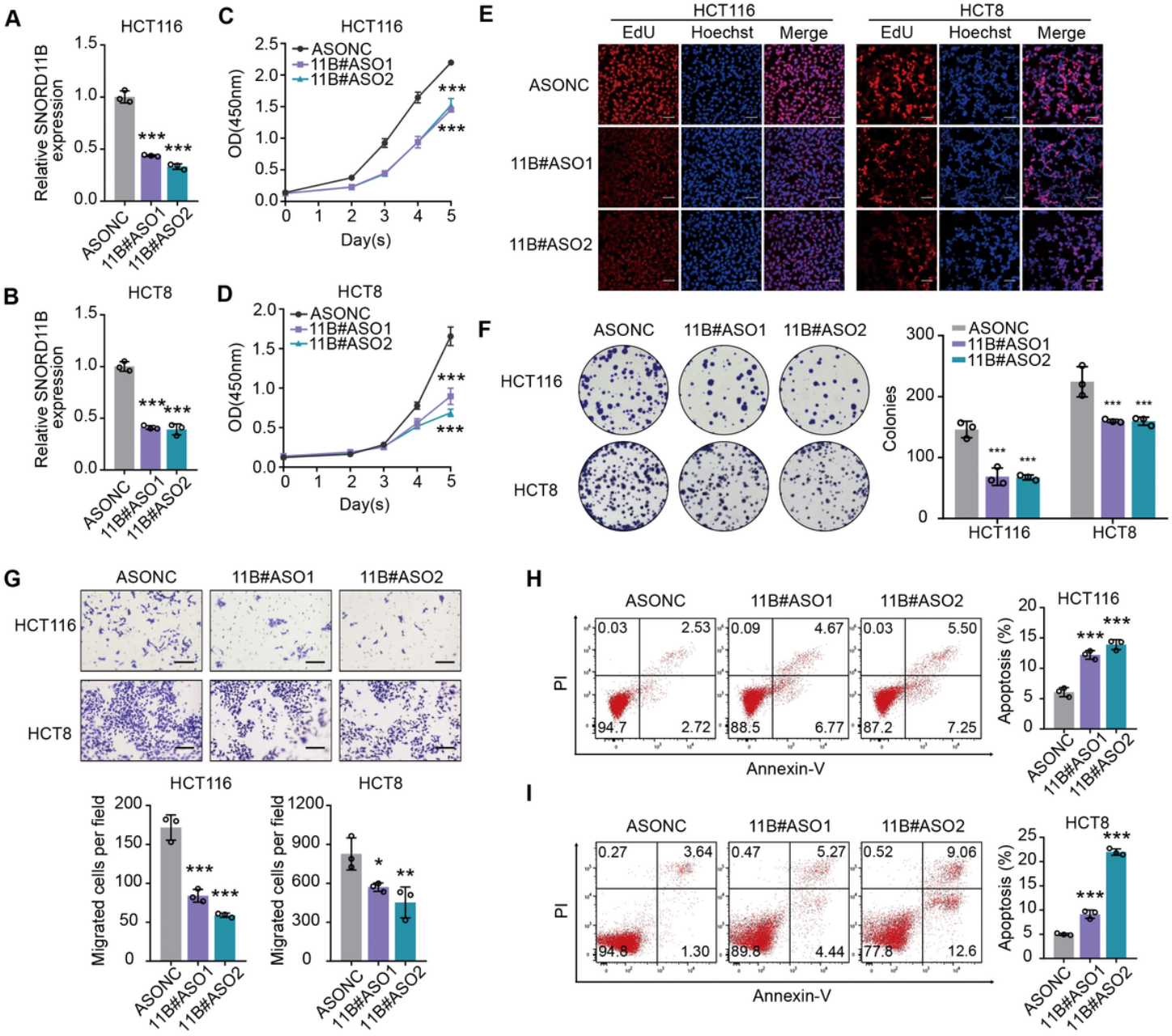

Figure 3

SNORD11B knockdown inhibits CRC malignancy *in vitro*. (A–B) Knockdown efficiency of ASOs against SNORD11B in HCT116 and HCT8 cells as determined by RT-qPCR. (C–F) Elevated proliferative activity of

CRC cells after SNORD11B silencing as determined by CCK-8 assay (C–D), EdU staining (scale bar: 50 μm) (E), and colony formation assay (F). (G) Invasion ability of CRC cells after SNORD11B silencing as detected by transwell assays (scale bar: 50 μm). (H–I) Apoptosis levels of SNORD11B-knockdown CRC cells as measured by flow cytometry.

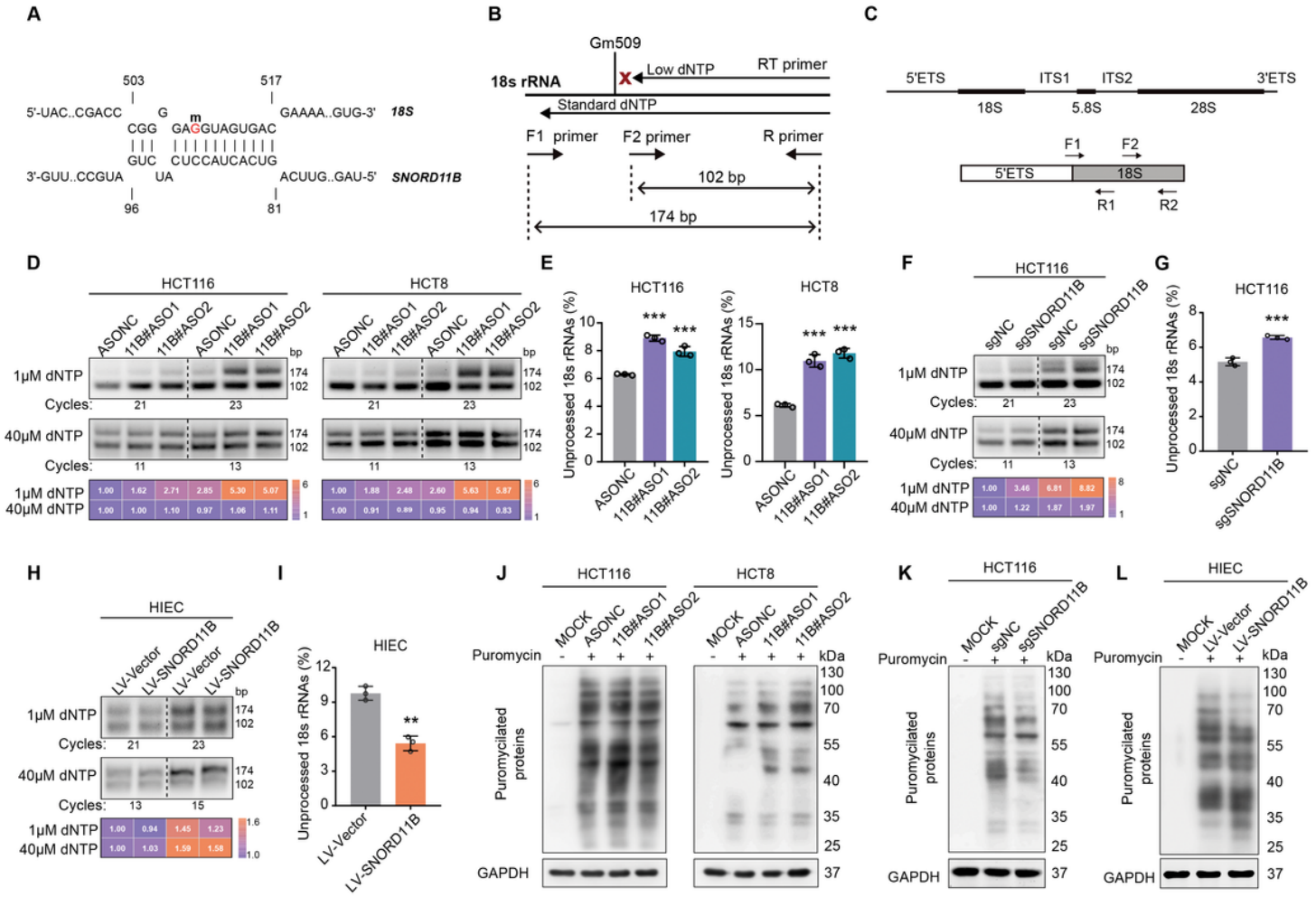

Figure 4

SNORD11B mediates Nm modification on G509 site of 18S rRNA. (A) Predicted interaction motif for the interaction between SNORD11B and 18S rRNA from snoRNA Atlas database. The G509 site, the Nm target, is shown in red. (B) Illustration of RTL-PCR method. See Materials and Methods section for detail. (C) Top: schematic diagram of the eukaryotic rRNA precursor. Bottom: specific primers for 18S rRNA precursor (primer pair F1/R1) and total 18S rRNA (primer pair F2/R2). (D, F, H) Decreased 18S rRNAs Nm modification activity at the G509 site after SNORD11B knockdown in HCT116 and HCT8 cells (D, F) and increased activity after SNORD11B overexpression in HIEC (H) as detected by RTL-PCR assay. (E, G, I) RT-qPCR results showing that knockdown of SNORD11B in HCT8 and HCT116 repressed 18S rRNA processing (E, G), whereas overexpression of SNORD11B in HIEC promoted 18S rRNA maturation (I). (J–L) Global protein synthesis in CRC cells with SNORD11B knockdown (J–K) and in HIEC cells with

SNORD11B overexpression (L) detected by puromycylation assay followed by western blotting. Expression of GAPDH was used as an internal reference.

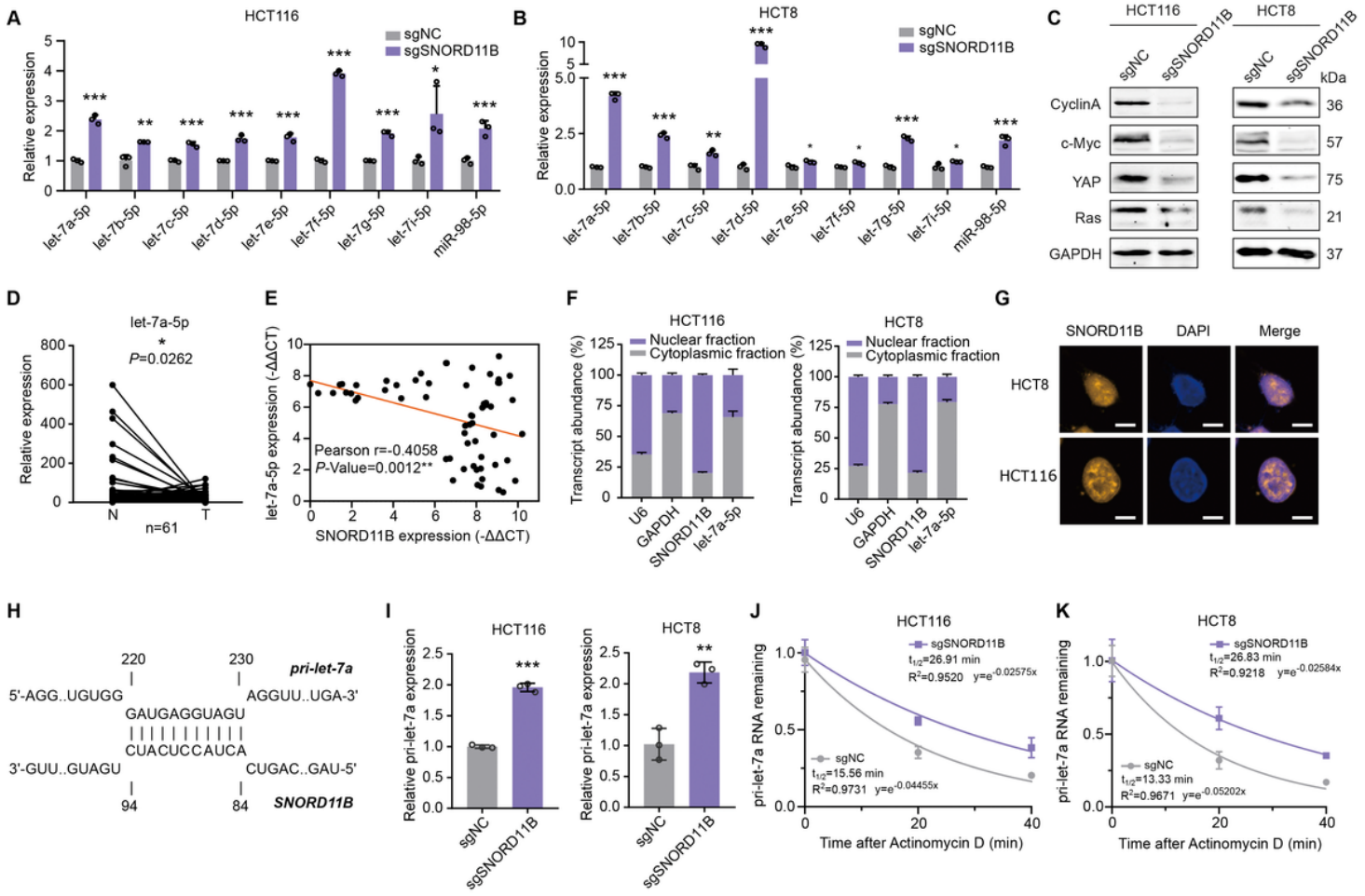

Figure 5

SNORD11B negatively regulates let-7-family miRNA expression. (A–B) Expression levels of let-7-family miRNAs after SNORD11B knockdown as detected by RT-qPCR. (C) Results of western blot assay showing expression of genes targeted by let-7-family miRNAs after SNORD11B knockdown. (D) Expression levels of let-7a-5p in paired CRC tissues (n=61) as measured by RT-qPCR. N, normal tissues; T, tumor tissues (paired-samples t-test). (E) Linear correlation analysis between SNORD11B and let-7a-5p expression in paired CRC tissues (Pearson's correlation analysis). (F) Expression levels of SNORD11B, let-7a-5p, cytoplasmic control transcripts (GAPDH), and nuclear control transcript (U6 snRNA) determined by RT-qPCR in the cytoplasmic and nuclear fractions of CRC cells. (G) Representative FISH images showing the expression of SNORD11B in HCT116 and HCT8 cells (scale bar: 5 μm). (H) Predicted interaction motif for the interaction between SNORD11B and pri-let-7a. (I) Expression levels of pri-let-7a after SNORD11B knockdown as detected by RT-qPCR. (J–K) RNA stability of pri-let-7a in CRC cells with SNORD11B knockdown as detected by RT-qPCR. Cells were treated with 10 μg/ml actinomycin D for the indicated times.

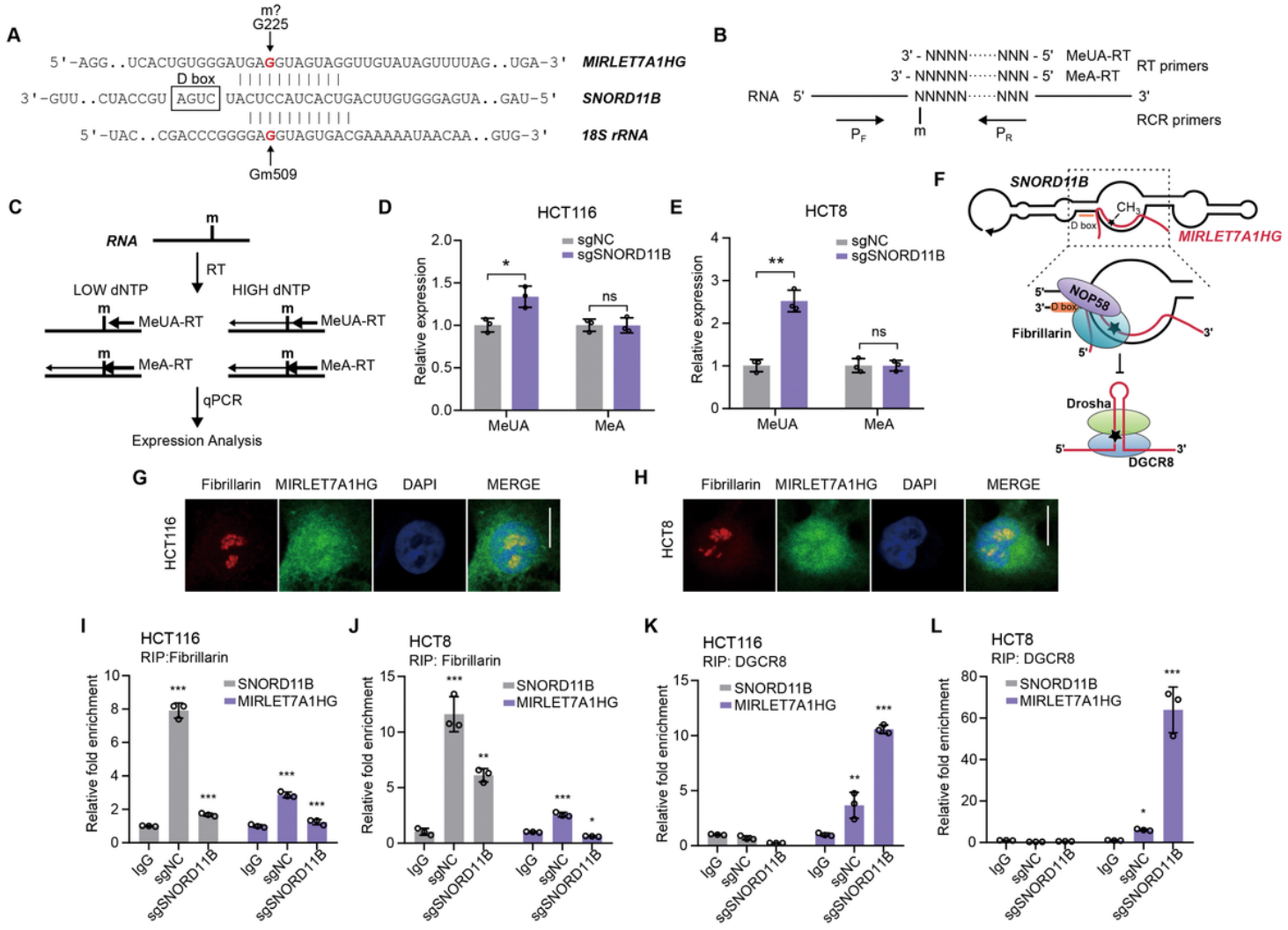

Figure 6

SNORD11B mediated Nm modification on G225 site of MIRLET7A1HG. (A) Predicted interaction motif for the interaction between MIRLET7A1HG/18S rRNA and SNORD11B. The underlying Nm target is shown in red. (B) Schematic diagram of the specific primer designed for the RT reaction and PCR. MeUA-RT, methylated site unanchored primer; MeA-RT, methylated site anchored primer; N, any nucleotide base. (C) Illustration of the RTL-qPCR procedure used to detect the exact location of the Nm modification. See the Materials and Methods section for detail. (D–E) qPCR results with the primer pair PF/PR used to amplify the MeUA-RT cDNA and MeA-RT cDNA generated from control and SNORD11B-knockdown cells. (F) Schematic diagram of the mechanism by which SNORD11B regulated the Nm modification on MIRLET7A1HG, resulting in splicing inhibition. (G–H) Representative FISH and IF images showing the co-localization of FBL and MIRLET7A1HG in HCT116 and HCT8 cells (scale bar: 10 μm). (I–L) RIP assays were performed using anti-FBL (I–J) and anti-DGCR8 (K–L) antibodies, and specific primers were used to detect the enrichment of SNORD11B and MIRLET7A1HG with RT-qPCR.

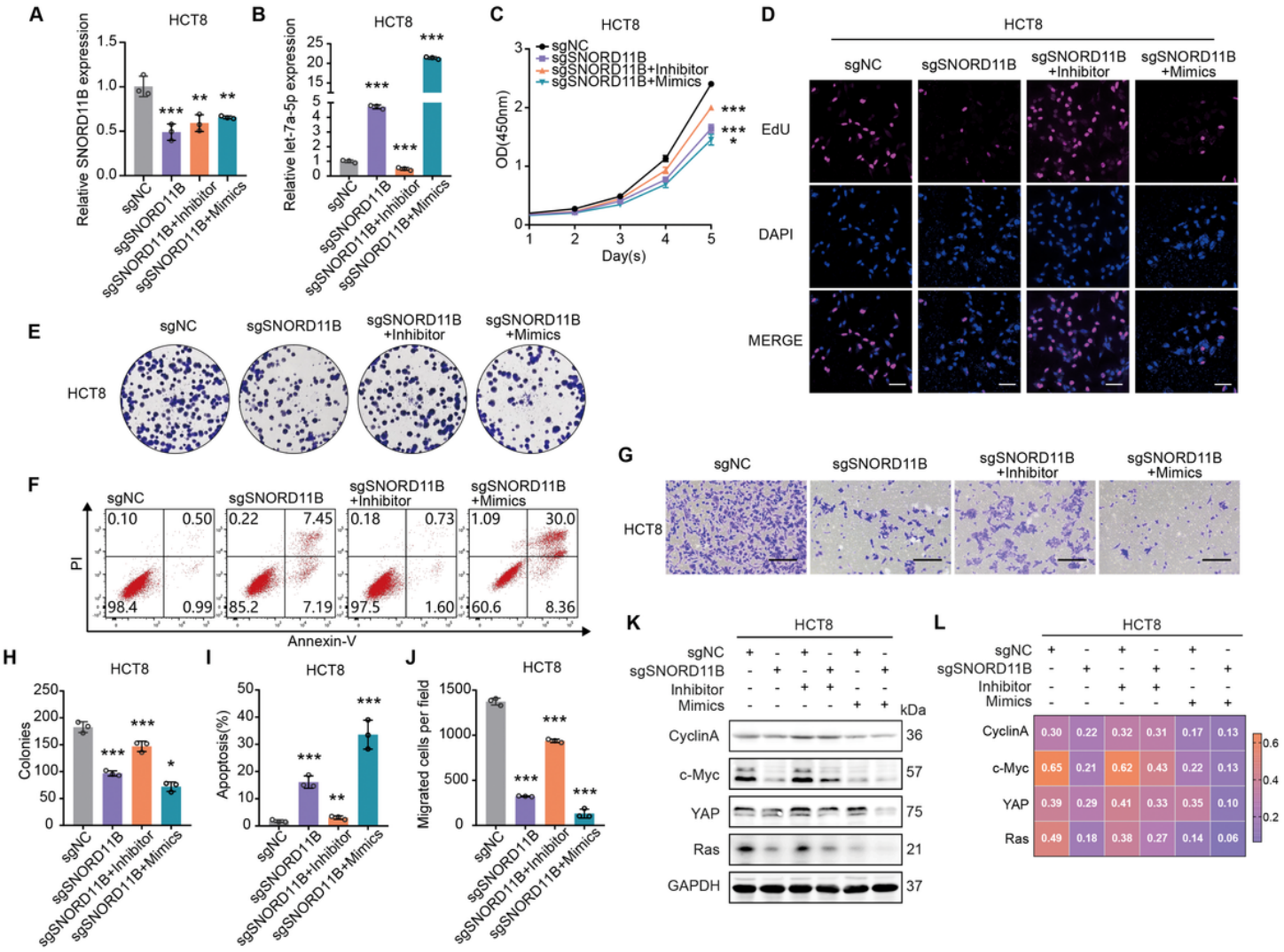

Figure 7

The oncogenic role of SNORD11B in CRC depends on let-7a-5p. (A–B) Expression levels of SNORD11B (A) and let-7a-5p (B) in cells with stable SNORD11B knockdown transfected with mimic and inhibitor for let-7a-5p as detected by RT-qPCR. (C–E, H) Elevated proliferative activity of cells with stable SNORD11B knockdown transfected with mimic and inhibitor for let-7a-5p as detected by CCK-8 assay (C), EdU staining (scale bar: 50 μm) (D), and colony formation assay (E, H). (F–J) Apoptosis levels (F, I) and invasion ability (G, J) of CRC cells with the indicated treatments, as measured by flow cytometry assays and transwell assays (scale bar: 50 μm), respectively. (K–L) Results of western blot assay to detect the expression of genes targeted by let-7-family miRNAs in cells with stable SNORD11B knockdown transfected with mimic and inhibitor for let-7a-5p.

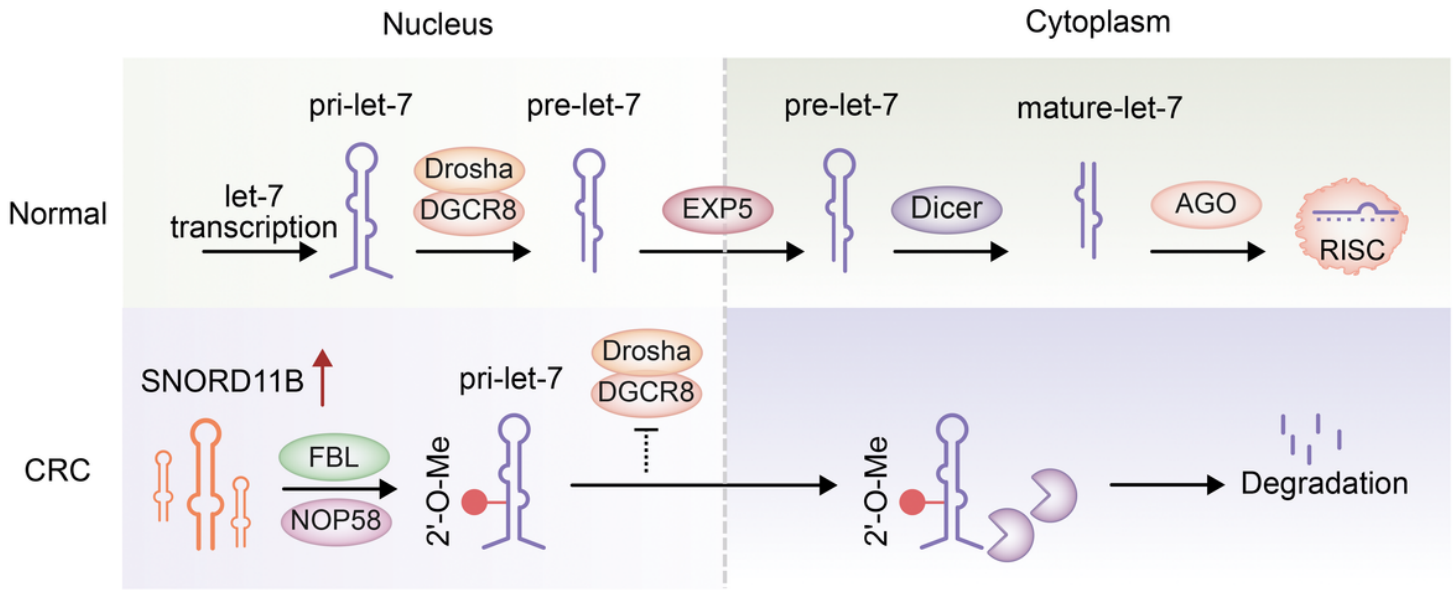

Figure 8

Proposed model.

Our findings suggest that SNORD11B mediates Nm modification of pri-let-7 so as to promote pri-let-7 degradation and attenuate the binding of the DGCR8/DROSHA complex to pri-let-7, thereby inhibiting splicing of pri-let-7 in the nucleus, reducing levels of let-7 in the cytoplasm.

Supplementary Files

This is a list of supplementary files associated with this preprint. Click to download.

- Supplementarymaterialsandmethods.docx